A simple Analytical model for solidification cooling rate based on the local heat flux density

M. Alizadeh[1]* and S.A. Jenabali-Jahromi[2]
[1]*Department of Metals, International Center for Science, High Technology & Environmental Sciences,Kerman,Iran.*
[2]*Department of Materials Science and Engineering, Shiraz University, Shiraz, Iran.*

Abstract
A new simple analytical model for prediction of cooling rate in the solidification process based on the local heat flux density extracted during solidification is introduced. In the modeling procedure, a solidifying control volume is considered in the mushy zone in which a heat balance equation is used to derive the present model. As the local heat flux density is a measurable parameter, the present model can be used directly on a production line. The present model was validated with numerical method and well adopted with analytical model of Garcia et al. The validation depicted that the present model can predict the cooling rate during solidification process with the same accuracy of the numerical method and Garcia's model. Moreover, it was shown that the present model can be used to calculate the average and local cooling rate, where the available models face some difficulties.

Keyword: Cooling rate, Local heat flux, Solidification, mushy zone

1. Introduction
One of the main parameters which affect the properties of cast metal ingots such as solute segregation, final distribution of inter-dendritic phases, secondary dendrite arm spacing, and hot tearing is the cooling rate in the mushy zone during solidification [1-11]. Usually numerical simulations of solidification are used to calculate the cooling rate and its variations along the mushy zone as a function of operational parameters [12-16]. However, a suitable analytical model can be very useful for quick analysis of the cooling rate. Garcia et al. developed an analytical heat transfer model describing the displacement of the solidus and liquidus isotherms and the temperature distribution in melt/mold system in a unidirectional solidification of binary alloys. The analytical model of Garcia et al. can determine the tip cooling rate (*CR*) as a function of parameters of the metal/mold system (such as the thermal diffusivities of mold and solidus/melt temperatures). This model can be described as follows [13, 17-19]:

$$CR = \frac{m(T_p - T_l)}{\sqrt{\pi}\ \alpha_{sl}\,\phi_2\,[1-erf(m\phi_2)]\exp(m\phi_2)^2} V_l^2 \quad (1)$$

In which

$$V_l = \frac{2\alpha_{sl}\,\phi_2^2}{\left[\dfrac{2\,k_s\phi_2\,(T_s - T_0)}{n\sqrt{\pi}\,(T_l - T_0)\exp(\phi_1^2)[M + erf(\phi_1)]h}\right] + S_l} \quad (2)$$

Where T_s is the non-equilibrium solidus temperature, T_0 the environment temperature, T_l the liquidus temperature and T_p the initial melt temperature. M implies the ratio of heat diffusivities of solid and mold material $(k_s c_s \rho_s / k_M c_M \rho_M)^{0.5}$, α_s and α_l present the solid and liquid thermal diffusivity, respectively ($k_s/c_s\rho_s$ and $k_l/c_l\rho_l$) and α_{sl} the mushy zone thermal diffusivity ($k_{sl}/c_{sl}\rho_{sl}$) which is calculated as described in the reference [13]. m indicates the square root of ratio of thermal diffusivities of mushy zone and liquid $(\alpha_{sl}/\alpha_l)^{0.5}$, n implies the square root of the ratio of thermal diffusivities of solid metal and mushy zone $(\alpha_s/\alpha_{sl})^{0.5}$ and h the heat transfer coefficient (W/m^2K). The terms ϕ_1 and ϕ_2 are solidification constants associated with the displacement of the solidus and liquidus isotherm and are determined by the simultaneous solution of below equations:

$$\frac{T_l - T_s}{erf(\phi_2) - erf(n\phi_1)} = \frac{k_s \exp[(n^2-1)\phi_1^2]}{k_{sl}\,n\,\exp[M + erf(\phi_1)]}(T_s - T_0) \quad (3)$$

$$\frac{T_l - T_s}{erf(\phi_2) - erf(n\phi_1)} = \frac{k_l\,m\exp[(1-m^2)\phi_2^2]}{k_{sl}\,[1-erf(m\phi_2)]}(T_p - T_l) \quad (4)$$

The term S_l in Eq. 2, presented in the model of Garcia et al. is the position of liquidus isotherm from metal/mold interface and is calculated using the solidification time (t) as follows:

**Corresponding Author:*
Tel: +983426226611 Fax:+983426226617
Email: alizadeh@icst.ac.ir
Address: Department of Metals, International Center for Science, High Technology & Environmental Sciences, Kerman, Iran
1. Assistant Professor
2. Professor

$$t = \frac{S_l^2}{4\alpha_{sl}\phi_2^2} + \frac{L_0 S_l}{2\alpha_{sl}\phi_2^2} \quad (5)$$

Where L_0 is the thickness of total pre-existing adjunct to metal in the virtual system (solid and mushy) and is determined by the following equation:

$$L_0 = \frac{\phi_2}{n\phi_1} \times \frac{2k_s\phi_1(T_s - T_0)}{\sqrt{\pi}\,(T_l - T_0)\,\exp(\phi_1^2)[M + erf(\phi_1)]h} \quad (6)$$

Although it seems that the model of Garcia et al. considered many parameters, the multiplicity of the metal/mold parameters makes it a complex model. For example, calculation of ϕ_1 and ϕ_2 leads to a complicated computational procedure in the model. Moreover, the presence of many variables in this model would raise the errors in the computation process.

In fact, the solidus and liquidus isotherms positions and the temperature profiles in the mold, solid, mushy and liquid zones are dependent on the local heat flux density extracted during the solidification [20]. Furthermore, the thermal diffusivities of mold, solid, mushy and liquid zones determine the thermal resistivity against the heat extraction during solidification. So, using the local heat flux density instead of above mentioned parameters can not only decrease the variables significantly but also represent the mold/metal parameters and some operational parameters such as the casting velocity and cooling conditions in a continuous casting process [21]. Therefore, the main goal of the present research is to derive a simple analytical model for calculating the cooling rate through the mushy zone as a function of local heat flux density. Attempts were made to enable the new present model to predict the cooling rate corresponding to any temperature and at any solid fraction in the mushy zone while it keeps its simplicity. Hereinafter, the simple analytical cooling rate model introduced in this work is briefly called SACR.

2. Numerical Simulation of Solidification

In this research, to validate the present analytical models, a numerical simulation of solidification is developed. In the first step, it is necessary to choose a solidification system; hence, due to the importance of continuous casting (CC) process of steel, this process is chosen for numerical simulation. In order to investigate the chemical composition, four grades of steels with dissimilar carbon contents and similar alloying elements are chosen. The basic steel alloy is 1.32 wt% Mn, 0.28 wt% Si, 0.007 wt% P and 0.007 wt% S. The carbon contents are 0.08 (steel of S1), 0.12 (steel of S2), 0.16 (steel of S3), 0.3 (steel of S4), and 0.4 (steel of S5). Table 1 summarizes the operational parameters of CC process of steels.

In this work, the following assumptions were made in the numerical simulation of CC process of a steel bloom:

Table 1. Practical and solidification conditions used for the numerical simulation of bloom

sample	S1	S2	S3	S4
Wt% C	0.08	0.12	0.16	0.4
$T_{pouring}$ - °C	1550	1545	1540	1530
ΔH_m - J/kg	243000	258000	259000	252000
$\Delta T_w{}^T$ - °C	4.63	4.66	4.7	4.58
Mold dimensions - m	0.23 × 0.25			
Mold length - m	0.78			
V_C - m min^{-1}	0.75			
Mold level - %	85			
Q_{mold} -lit min^{-1}	2347			
$Q_{s\,1}$ - lit min^{-1}	23			
$Q_{s\,2}$ - lit min^{-1}	56			
$Q_{s\,3}$ - lit min^{-1}	33			
k_l - W/mK	39			
k_s - W/mK	$(21.6+8.35\times10^{-3}T)$			
ρ_l - kg m^{-3}	7965.98-0.619T			
ρ_s - kg m^{-3}	(8105.91-0.5091T)			
C_l - J/kgK	824.6157			
C_s - J/kgK	(429.849+0.1498T)			

a) Heat transfer along the transverse section of bloom is recognized as symmetry and along the bloom withdrawal direction is neglected.

b) The latent heat of steel solidification is converted into an equivalent specific heat capacity in the mushy zone [22-23].

c) The fluid flow is expected to affect thermal field via enhanced heat transfer and then an effective thermal conductivity is employed in the liquid core and mushy zone of bloom [24-25].

According to the forgoing assumptions, a two-dimensional unsteady state heat transfer equation is available as follows:

$$\rho(T)C'(T)\frac{\partial T}{\partial t} = k(T)\nabla^2 T = k(T)\left[\frac{\partial^2 T}{\partial x^2} + \frac{\partial^2 T}{\partial y^2}\right] \quad (7)$$

Where ρ is the temperature dependent density *(kg/m³)*, *C'* the temperature dependent equivalent heat capacity *(J/kg K)*, *T* the bloom temperature *(K)*, *t* the time *(s)*, *x* and *y* the rectangular coordinates *(m)* and *k* the temperature dependent thermal conductivity of steel *(W/m K)*. The equivalent heat capacity, *C'*, is determined by following expression [26]:

$$C'(T) = \begin{cases} C(T) & T < T_s \ \ or \ \ T > T_l \\ C(T) + \Delta H_m \dfrac{\partial f_s}{\partial T} & T_s \le T \le T_l \end{cases} \quad (8)$$

Where $C(T)$ is the specific heat of solid steel or liquid steel, which is a function of temperature, T_l is liquidus temperature of steel, T_s is solidus temperature of steel

and f_s is the solid fraction in the mushy zone. The term f_s is calculated as follows:

$$f_s = \frac{T - T_l}{T_s - T_l} \tag{9}$$

Boundary Conditions

The boundary condition for the surface of the strand is written as follows:

$$-k(T)\frac{\partial T}{\partial n} = q_e \tag{10}$$

Where n in the normal to the boundary and $\frac{\partial T}{\partial n} = \frac{\partial T}{\partial x}$ for $y = 0$ and $\frac{\partial T}{\partial n} = \frac{\partial T}{\partial y}$ for $x = 0$. The extracted heat (q_e in w/m^2) during CC process is calculated using separate models for mold, spray and radiation regions and is used as boundary conditions.

In the mold region [21]:

$$q_e = \frac{\alpha\, \Delta T_w^T\, \rho_w\, C_w\, Q_{mold}}{P_m} \times \frac{e^{-\alpha z}}{1 - e^{-\alpha H_{me}}} \tag{11}$$

where Q_{mold} is the volume cooling water rate (m^3/s), ρ_w is density of water (997 kg/ m3 at 25 °C), C_w is heat capacity of water $(4180\ J\ kg^{-1}\ at\ 25°C)$, P_m is perimeter of the tube mold (billet and bloom mold), z is mold length (starting from the meniscus) (m), α is slope of straight lines in a q_e-z half-logarithmic plot and its value used in this work is $1.5m^{-1}$, ΔT_w^T is total increase of the cooling water temperature $(°C)$ and the term H_{me} is the effective mold length which is in contact with the melt and is calculated by ($mold\ level \times H_m$) where H_m is the mold length (m).

In the spray cooling region [26]:

$$q_e = h_j (T - T_w) \tag{12}$$

Where the subscript j shows the number of spray cooling section. In the present research, the spray cooling zone is divided into 3 sections according to the flow rate of water. h_j is the convective heat transfer coefficient in the j^{th} section, which can be calculated as follows (in $kW/m^2\,^oC$):

$$h_j = h_{\alpha j} \cdot w_j^r + h_{r j} \tag{13}$$

Where $h_{\alpha j}$, r and $h_{r j}$ are the parameters of nozzle, for air-mist spray nozzle, $h_{\alpha j}$ is 0.35, r is 0.556 and $h_{r j}$ is 0.13. w_j (in $lit\ s^{-1}m^{-2}$) is the sprayed water densityand can be calculated by following formula:

$$w_j = \frac{Q_{s j}}{A_j} \tag{14}$$

Where A_j is the sprayed area of the j^{th} cooling section and $Q_{s j}$ is the spray water flow rate in the j^{th} cooling section.

In the Radiation cooling region [27]:

$$q_e = h_{Ra}(T - T_{amb}) \tag{15}$$

$$h_{Ra} = \sigma\, \varepsilon\, (T^2 + T_{amb}^2)(T + T_{amb}) \tag{16}$$

Where e is the emissivity of bloom surface (0.8), s the Stefan– Boltzman constant $(5.67 \times 10^{-8}\ W/m^2K^4)$, and T_{amb} is the ambient temperature (K).

The local heat flux density extracted from the solidifying steels is calculated by Eqs. 10-15 and is applied as boundary conditions in the numerical simulation of CC. Fig. 1 depicts the local heat flux density as a function of solidification time (or distance from meniscus) for samples S1-S4. The steps created in the local heat flux density curves is due to sudden changes in heat extraction rate from the strand surface as the strand moves from the mold to the sprays, from a spray zone to the next one or from the sprays to the radiation zone. These local heat flux densities also will be used in the SACR model in the next parts.

Fig. 2 depicts the numerically simulated shell thickness curves for steels of S1-S4. In fact, these curves show the position of isotherms coincident to $f_s=0$ and $f_s=1$ at any solidification time during CC process. In this work, these diagrams are used to determine the final length of mushy zone (L_m^f) as well as local solidification time (t_f). The calculation procedure t_f and corresponding L_m^f at any desired solidification time have been illustrated in Fig. 2. As this figure shows, the vertical distance between the lines of $f_s=0$ and $f_s=1$ determines L_m^f and the time required for the mushy zone to grow from $f_s=0$ up to $f_s=1$ (the horizontal distance) is equal to t_f. Table 2 lists t_f and corresponding L_m^f extracted from the shell thickness curves (Fig. 2) at some desired solidification times for the steels S1-S4.

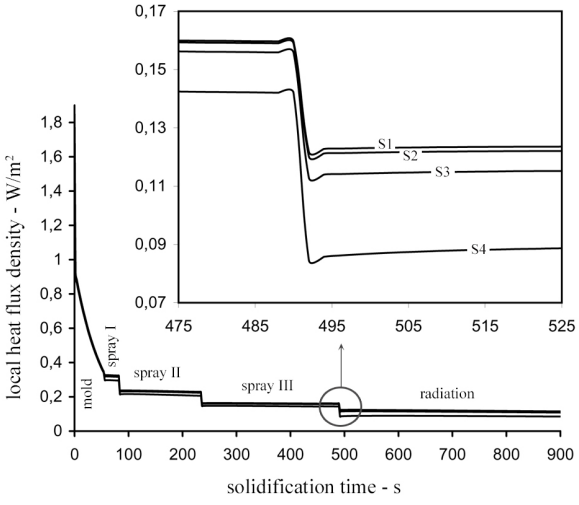

Fig. 1. The local heat flux density extracted during solidification calculated using analytical models

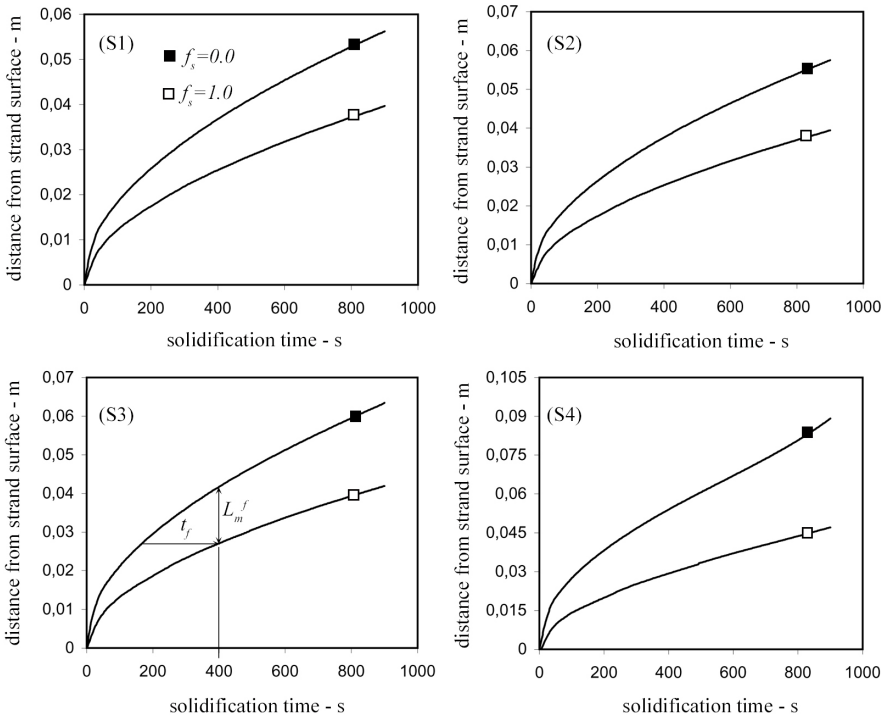

Fig. 2. The shell thickness curves corresponding to f_s=0 and f_s=1 simulated by the numerical simulation

Table 2. The local solidification time and final mushy zone length at any desired solidification time calculated using Fig. 2.

Solidification time -s	S1: 0.08 wt%C		S2: 0.12 wt%C		S3: 0.16 wt%C		S4: 0.4 wt%C	
	t_f - s	L_m^f - m	t_f - s	L_m^f - m	t_f - s	L_m^f - m	t_f - s	L_m^f - m
20	8	0.002449	9	0.00253	10	0.003185	12	0.005111
150	84	0.007392	89	0.008047	94	0.009638	112	0.016094
300	158	0.009919	166	0.010761	178	0.012726	216	0.021522
450	228	0.011977	242	0.0131	260	0.015439	318	0.026107
600	300	0.013662	315	0.014784	338	0.017592	412	0.030037
750	368	0.015159	390	0.016562	418	0.019557	506	0.03359
900	436	0.016562	462	0.018059	496	0.021522	615	0.038107

3. Procedure of SACR modeling

The following concepts and assumptions are considered to derive the SACR model:

a) During solidification of the melt, the heat extraction changes the energy of the materials in two ways: 1-There is a decrease in the enthalpy of the liquid or solid due to cooling which is known as sensible heat. 2-There is a decrease in the enthalpy due to liquid/solid and solid/solid transformation which is known as latent heat.

b) The heat extracted during solidification process, must pass through several thermal resistance such as liquid wall, mushy wall, solidified shell, interfacial resistance (mold powder layer and air gap in the mold region and oxide layer below the mold in CC process) and the mold wall [28-29]. Fig. 3.a depicts the thermal resistance against the heat transfer during solidification (mold region in CC process). According to these assumptions, these thermal resistances act as series wall.

c) The solid/solid latent heat is ignored.

d) Based on the assumption b and c, it would be possible to suppose that the heat extracted from the mushy zone is equal to the heat passing through the solidified shell, the interfacial resistance, and the mold.

Let us consider a control volume in the mushy zone including a dendrite with the length of L_m^f and liquid surrounding it (Fig. 3(b)). According to the above assumptions, the heat balance equation in the solidifying control volume could be written as follows:

$$q_e\left(\frac{A}{V}\right) = -\rho C_p\left(\frac{dT}{dt}\right) + \rho \Delta H_m\left(\frac{df_s}{dt}\right) \qquad (17)$$

Where the term A (in m^2) is the surface area of heat

transfer and the term V (in m^3) represents the volume of solidifying control volume.

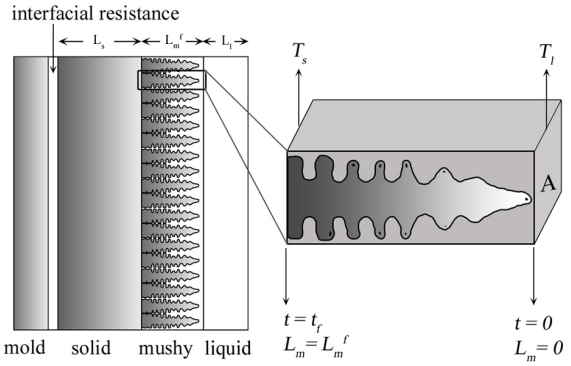

Fig. 3. (a)The schematic illustration of thermal resistances against heat withdrawal during a solidification process and (b) the solidifying volume in the mushy zone.

In fact, the above equation represents the heat balance during growth of a dendrite (or a mushy wall) form $L_m = 0$ (at $t = 0$, $T = T_l$ and $f_s=0$) to $L_m = L_m^f$ (at $t = t_f$, $T = T_s$ and $f_s=1$) where the term of L_m (in m) is the time dependent length of mushy zone, t, T, and f_s are the time (in s), temperature (in ^oC) and solid fraction through the solidifying control volume, respectively. According to Fig. 3(b), when the solidification in the control volume is done, the terms of t, f_s, and T vary between 0-t_f, 0-1, and T_l-T_S respectively. As can be seen from Fig. 3(b), the left side of control volume is corresponding to T_s and the right side of it has been located at T_l. In other words, the term f_s at the right side of control volume is equal to zero and at the left side of it is equal to one. The terms ρ and C_p represent density and specific heat of mushy zone, respectively and the term ΔH_m is the latent heat of fusion.

Although the term cooling rate (dT/dt) has been presented in Eq. 17, we cannot use it to calculate the cooling rate; because it is difficult to compute the term (df_s/dt) as a function of operational parameters.

According to Fig. 3(b) it can be possible to write the term A/V as follows:

$$\frac{A}{V} = \frac{A}{A L_m} = \frac{1}{L_m} \tag{18}$$

It would also be possible to express the term L_m as a function of t using a parabolic growth rate relationship [30] where:

$$L_m = \Phi \sqrt{t} \tag{19}$$

Substituting Eqs.18 and 19 in Eq. 17 leads to the heat balance equation as a function of t:

$$\frac{q_e}{\Phi} t^{-\frac{1}{2}} = -\rho\, C_p \left(\frac{dT}{dt}\right) + \rho\, \Delta H_m \left(\frac{df_s}{dt}\right) \tag{20}$$

Due to the terms t and df_s/dt, the above equation cannot be useful to calculate the cooling rate (dT/dt). Therefore, it can be written as:

$$\frac{q_e}{\Phi} t^{-\frac{1}{2}} = -\rho\, C_p \left(\frac{dT}{dt}\right) + \rho\, \Delta H_m \left(\frac{df_s}{dT} \times \frac{dT}{dt}\right) \tag{21}$$

Multiplying above equation in the term dt, gives the heat balance by following equation:

$$\frac{q_e}{\Phi} t^{-\frac{1}{2}} dt = -\rho\, C_p\, dT + \rho\, \Delta H_m \left(\frac{df_s}{dT} dT\right) \tag{22}$$

Advantage of above equation (22) is separating the temperature dependant terms and the time dependant terms. Also, the term df_s/dt has been replaced by the term df_s/dT which makes the equation simpler to compute.

When dependency of ρ and C_p on temperature is ignored, integration of Eq. 22 in the time range of 0 - t and temperature range of T_l - T gives:

$$\left(\frac{2 q_e}{\Phi}\right)(t)^{\frac{1}{2}} = -\rho\, C_p (T - T_l) + \rho\, \Delta H_m f_s \tag{23}$$

So, it is possible to derive a correlation for the cooling rate (dT/dt) in the mushy zone as a function of local heat flux density which is independent of variable time t in the mushy zone. For this purpose, it is necessary to extract the temperature (T) versus the time (t) and then calculate the dT/dt. However, extraction of heat T vs. t is not too simple to calculate dT/dt ; therefore, it is necessary to calculate t vs. T by the following equation:

$$t = \frac{\Phi^2}{4 q_e^2} \left[-\rho\, C_p (T - T_l) + \rho\, \Delta H_m f_s\right]^2 \tag{24}$$

Hence, the drive of the inverse of cooling rate can be implied by Eq. 25:

$$\frac{dt}{dT} = \frac{\Phi^2}{4 q_e^2} \times 2 \times \left[-\rho\, C_p + \rho\, \Delta H_m \frac{df_s}{dT}\right] \times \left[-\rho\, C_p (T - T_l) + \rho\, \Delta H_m f_s\right] \tag{25}$$

Finally, it is enough to reverse the above equation and derive the Cooling Rate (CR) equation as follows:

$$CR = \frac{dT}{dt} = \frac{2 q_e^2}{\Phi^2\, C' \Delta h'} \tag{26}$$

Where the term C' (in $j/m^3/^oC$) is called apparent volumetric specific heat and the term $\Delta h'$ (in j/m^3) is called apparent volumetric latent heat defined in the present work by Eqs. 27 and 28:

$$C' = \rho \left(-C_p + \Delta H_m \frac{df_s}{dT}\right) \tag{27}$$

$$\Delta h' = \rho \left(-C_p (T - T_l) + \Delta H_m f_s\right) \tag{28}$$

Eq.26 expresses the SACR (in $^oC/s$) model and can calculate the solidification cooling rate at any solid fraction and corresponding temperature. If $f_s=1$, the cooling rate is calculated over the temperature interval between T_l and T_s which is known as average cooling rate through the mushy zone.

Mathematical modeling of Φ

For modeling the term Φ (in $m/s^{0.5}$), the dendrite velocity during solidification process through a control volume can be used. According to Fig. 3(b), it can be imaged that a dendrite moves (in a control volume) from $L_m=0$ to $L_m = L_m^f$ in the time duration of t_f, therefore, an average velocity (v_m in m/s) is considered for a dendrite as follows:

$$v_m = \frac{L_m^f}{t_f} \tag{29}$$

When the liquidus isotherm is the interface between the liquid zone and mushy zone, it would be possible to calculate the growth velocity of mushy zone by using a simple heat flux Eq. 31:

$$\rho\,\Delta H_m\, v_m = k_{mushy} G_{mushy} - k_l G_l \tag{30}$$

Where G_l ($^oC/m$) is the thermal gradient of fully liquid zone and G_{mushy} ($^oC/m$) is the thermal gradient of mushy zone. The mushy zone (as a thermal wall) is a mixture of liquid and solid. So, its conductivity (k_{mushy}) is replaced by an equivalent thermal conductivity which is calculated by $k_{mushy} = k_s f_s + B k_l (1-f_s)$ in which the term B is a constant number for consideration of turbulence in superheated melt and varies between 2 and 7 [32]. Combination of Eqs.29 and 30 gives the local solidification time:

$$t_f = L_m^f \times \frac{\rho\,\Delta H_m}{k_{mushy} G_{mushy} - k_l G_l} \tag{31}$$

As mentioned before, when $t=t_f$, the mushy zone length would be equal to L_m^f. Thus, we can write Eq.19 for $t = t_f$ as follows:

$$L_m^f = \Phi \sqrt{t_f} \tag{32}$$

Extracting the term of t_f from Eq.32 and substitution of it in Eq.31 give the term Φ by Eq. 33:

$$\Phi = \left[L_m^f \times \frac{k_{mushy} G_{mushy} - k_l G_l}{\rho\,\Delta H_m} \right]^{\frac{1}{2}} \tag{33}$$

When the mushy zone is considered as a thermal wall, the term L_m^f can be calculated by using Fourier heat transfer equation. Hence, the L_m^f can be written as:

$$L_m^f = -k_{mushy} \frac{T_l - T_s}{q_e} \tag{34}$$

The thermal gradient of mushy zone and fully liquid zone presented in Eq. 33 are also calculated by using Eqs. 35 and 36:

$$G_{mushy} = \frac{T_l - T_s}{L_m^f} \tag{35}$$

$$G_l = \frac{T_p - T_l}{L_l} \tag{36}$$

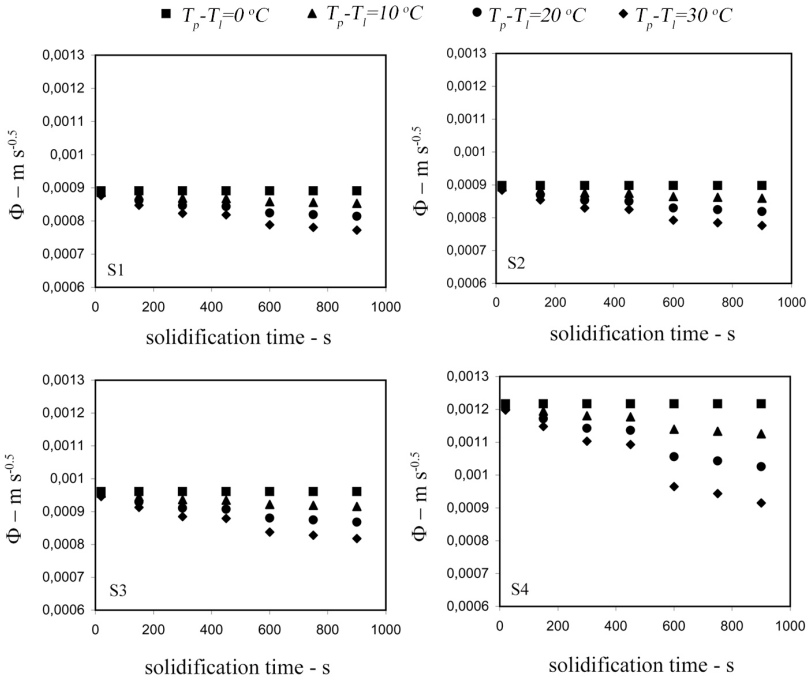

Fig. 4. Variation of Φ *with solidification time in various values of* ($T_p - T_l$)

The term T_p is the pouring temperature and the term L_l is the length of fully liquid zone (see Fig. 3(a)). To calculate the term L_l , if half of casting wide is considered as W, then according to Fig. 3.a the following equation can be written for the length of fully liquid zone:

$$L_l = W - L_s - L_m^f \tag{37}$$

The term L_s (in *m*) represents the fully solidified shell thickness and is calculated as follows:

$$L_s = K\sqrt{t_s} \tag{38}$$

Where t_s is the solidification time (in *s*) and K is a constant which is determined by experiment or numerical simulation work, and this can be a limitation in calculation of Φ. Moreover, determination of L_m^f is not possible easily by analytical method. Therefore, in the next part, the challenge is to simplify Eq. 33.

Simplification of Φ

The term T_p, represented in Eq.36, is supposed to be constant during calculation of Φ using Eq.33. In other words, Eq.33 calculates the term Φ with a constant temperature difference of (T_p – T_l). Fig. 4 shows variation of Φ with solidification time in various values of (T_p – T_l) for all of the steels under CC process.

Actually, in a casting process, the melt temperature difference is decreased by increasing the solidification time (because the temperature of melt center is decreased) and according to Fig. 4, when the melt temperature difference is decreasing; the term Φ is decreased, too. Moreover, dependency of Φ on the solidification time became more invisible. Also, Fig. 4 reveals that in the initial stages of solidification (where practically the melt temperature difference has a considerable value) the term Φ does not change significantly with the melt temperature.

Based on the above explanations, it would be possible to neglect the thermal gradient of fully liquid zone in comparison to the thermal gradient of mushy zone. Fig. 5 compares the terms of G_l and G_{mushy} calculated by Eqs.35 and 36 for the sample of S3.

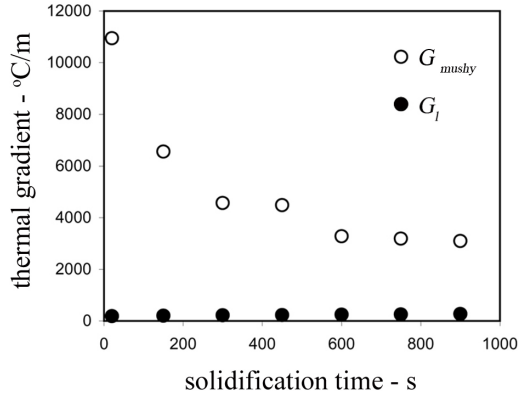

Fig. 5. Comparison between the terms of G_l and G_{mushy} for CC of steel of S3

This figure confirms that the term G_l is noticeably lower than the term G_{mushy}; therefore, it can be possible to ignore the term G_l in comparison to G_{mushy}.

Elimination of G_l and replacement of G_{mushy} with Eq.35 changes Eq.33 as follows:

$$\Phi = \left[\frac{k_{mushy}(T_l - T_s)}{\rho\,\Delta H_m}\right]^{\frac{1}{2}} \tag{39}$$

In fact, this equation represents the simplified form of Eq.33 which is independent of the terms L_m^f and L_l.

4. Model Validation

Validating the model of Φ

As already shown, the final length of the mushy zone is related to the local solidification time by the term Φ (see Eq.32). The result of CC simulation shows (see Table 2) the variation of L_m^f versus t_f that has been plotted in Fig. 6 as well. This figure indicates that the power form trend line is fitted on the simulated data. Comparing the fitted equations (showed on the top of Fig. 6) with Eq.32 confirms, with a good approximation, the term L_m^f is proportional to root square of t_f , and this result is in agreement with the one expressed in Eq.32.

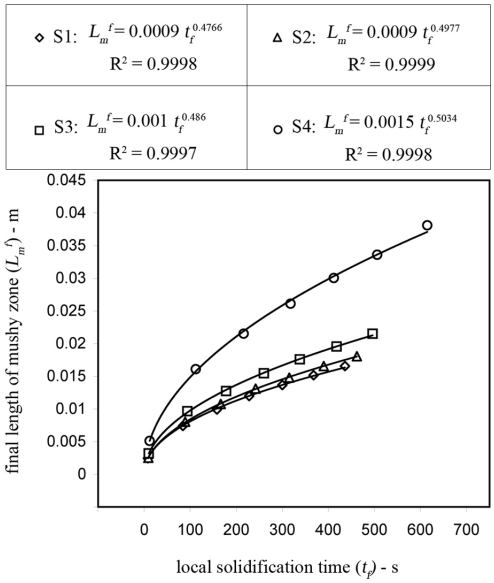

Fig. 6. Variation of simulated L_m^f versus t_f with together the power form equations fitted on them

Another result of Fig. 6 is the simulated term Φ for any steel alloy. In fact, coefficient of t_f (in the equations listed above the Fig. 6) is the term Φ (compare with Eq. 32). Table 3 compares the simulated term Φ with those predicted by the present analytical model (Eq. 39). As can be seen, both simulated and analytical predictions are in a good agreement. In fact, the results listed in Table 3 validate Eq.39 and they can be used as the analytical expression for the term Φ. However, the existence of some approximations in both models caused a small difference between them.

Table 3. Comparing the simulated term of Φ with that one predicted by the present analytical model (Eq.39)

Alloy	The term of Φ - m/s$^{0.5}$		Error%
	Simulated	Predicted by Eq.39	
S1: 0.08 wt%C	0.0009	0.000891	1
S2: 0.12 wt%C	0.0009	0.000898	0.2
S3: 0.16 wt%C	0.001	0.000961	3.9
S4: 0.4 wt%C	0.0015	0.001217	18.8

Validation of SACR model

a- Comparison with the simulated results

In this part, the cooling rate of strand (produced through the CC process) was calculated by the present analytical model and compared with the results of Eq.40 in which the term of t_f is determined by simulation of CC process (see Table 2).

$$CR = \frac{T_l - T_s}{t_f} \tag{40}$$

Since the Eq.40 calculates the average cooling rate in the mushy zone, the ability of the present analytical model for calculating the average cooling rare would also be checked. As mentioned before, in the present CC simulation, the term f_s is determined by the linear model (see Eq. 9); therefore, the SACR model also must be applied with the linear model f_s. So, the term df_s/dT presented in Eq. 27 is calculated as follows:

$$\frac{df_s}{dT} = \frac{1}{T_s - T_l} \tag{41}$$

Fig. 7 compares the results of SACR model with those results of Eq. 40. As can be seen, the cooling rate calculated by both methods behaves in a similar trend. Also, there is an acceptable agreement between them. However, some approximations (for example in the calculation of the extracted heat) and simplifying assumptions in both models cause a reasonable mismatching between them.

b- Comparison with the analytical model of Garcia et al.

Another way to assess the validity of the SACR model is to compare its results with those of Garcia's model. Since Garcia's model is a local cooling rate model (at $f_s=0$), the ability of SACR model for calculating the local cooling rate also would be checked. As mentioned before, in SACR model, the latent heat is released according to the solid fraction at a particular temperature (T). In other words, the cooling rate calculated by SACR model is dependent

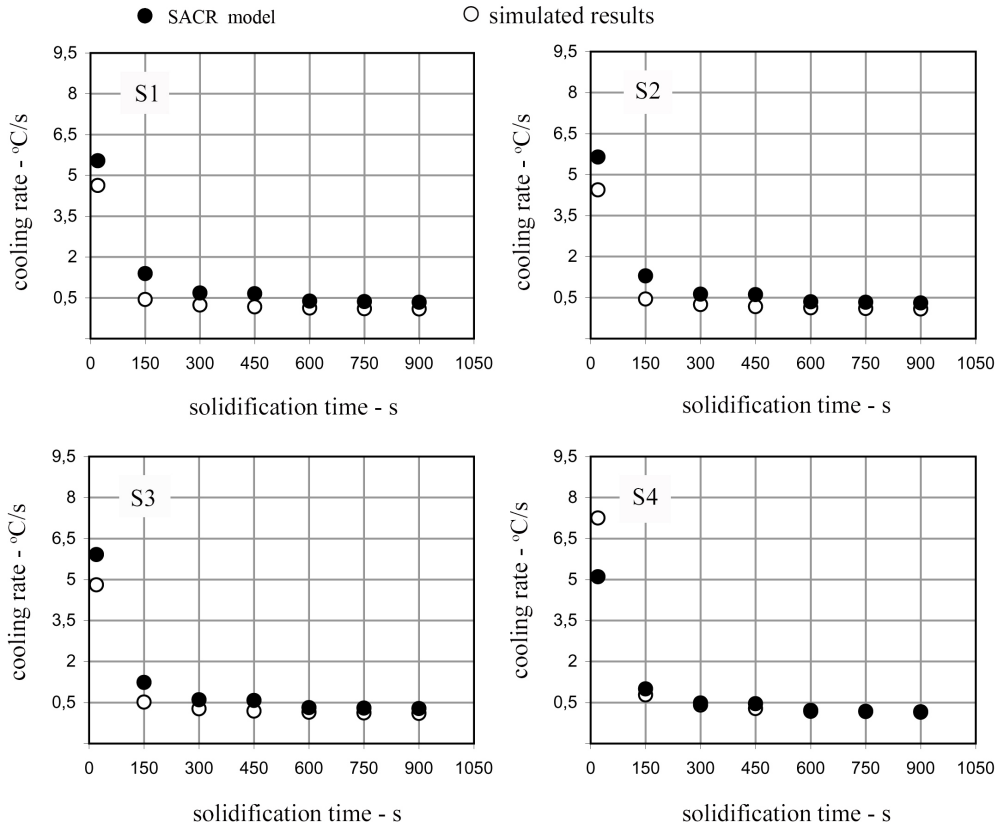

Fig. 7. Comparison between the cooling rate data calculated by 1-Eq.40 (aided by simulation) and 2-SACR model

$$f_s = \frac{1}{1-k_0}\left(\frac{T-T_l}{T-T_f}\right) \quad \& \quad \frac{df_s}{dT} = \frac{1}{1-k_0} \times \frac{T_l - T_f}{(T-T_f)^2} \tag{42}$$

$$f_s = 1-\left(\frac{T-T_f}{T_l-T_f}\right)^{\frac{1}{k_0-1}} \quad \& \quad \frac{df_s}{dT} = -\frac{1}{k_0-1} \times \left(\frac{1}{T_l-T_f}\right) \times \left(\frac{T-T_f}{T_l-T_f}\right)^{\frac{2-k_0}{k_0-1}} \tag{43}$$

$$f_s = 1-\left(\frac{T-T_s}{T_l-T_s}\right)^2 \quad \& \quad \frac{df_s}{dT} = -2 \times \left(\frac{1}{T_l-T_s}\right) \times \left(\frac{T-T_s}{T_l-T_s}\right) \tag{44}$$

on the relationship between the solid fraction and temperature. Eqs. 41-43 represent some models for calculating the solid fraction and their derivatives with respect to the temperature (Eq.42: Lever rule, Eq. 43: Scheils's, equation and Eq.44: quadratic model). These equations have been used in SACR model separately and their results are compared with the analytical model of Garcia et al.

Where T_f is the fusion temperature (1536 ^oC) and the term k_0 is the equilibrium partition ratio and is calculated as $k_0 = (T_f-T_l)/(T_f-T_s)$. The heat transfer coefficient required in Garcia's model is calculated by Eq.13 through the solidification time. Fig. 8 shows the variation of h versus the solidification time. The term h can be written as a function of solidification time (t_s) using the trend line as shown in Fig. 8.

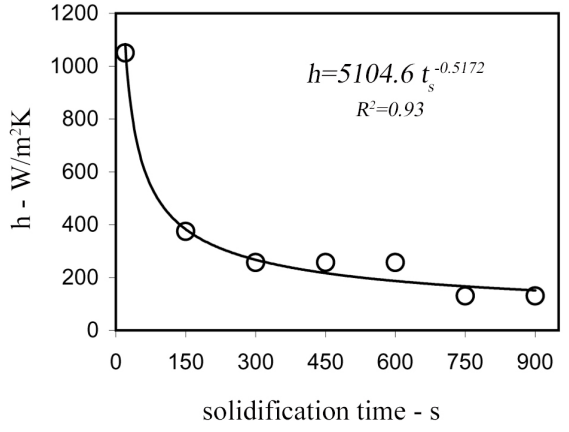

Fig. 8. Variation of heat transfer coefficient against the solidification time calculated by Eq.13

Fig. 9 compares the cooling rates calculated by both SACR model (with three types of f_s) and Garcia's model. For more clarification, those parts of diagrams which are related to the solidification time above than 400s are plotted again. The cooling rates emerged by SACR model behave similarly to results of Garcia's model for all steels. Fig. 9 depicts that at the tip of the mushy zone (when $f_s=0$ and $T=T_l$), at any solidification time, the Schiels's equation and Lever rule lead to equal values of cooling rate calculated with the SACR model and have most coincidence with the results of Garcia's model. When the quadratic model of f_s is used in the SACR model, the calculated cooling rates have a considerable difference (approximately twice at solidification times more than 150 s) with the results of Garcia's model.

5. Conclusions

In the present work, a novel analytical model has been introduced for the cooling rate during solidification. The present model is based on the local heat flux density extracted during solidification process. The following main conclusions can be drawn from the present work:

- The results of model validation reveal that the present analytical model can be used as well as the numerical simulation and analytical models.
- The term q_e existing in present analytical model represents the operational parameters (for example, in the CC process, casting velocity, and cooling conditions) therefore; it considers the role of operational parameters in cooling rate values.
- The present analytical model calculates cooling rate using the determinable parameters; for example, this model is not a function of local solidification time.
- The present analytical model can be used to calculate the average and local cooling rate at any solid fraction in the mushy zone.
- The cooling rate calculated by the present model is dependent on the relationship between the solid fractions with the temperature.
- Depending on the model of solid fraction and solidus temperature, both equilibrium and nonequilibrium cooling rates can be calculated by the present analytical model.

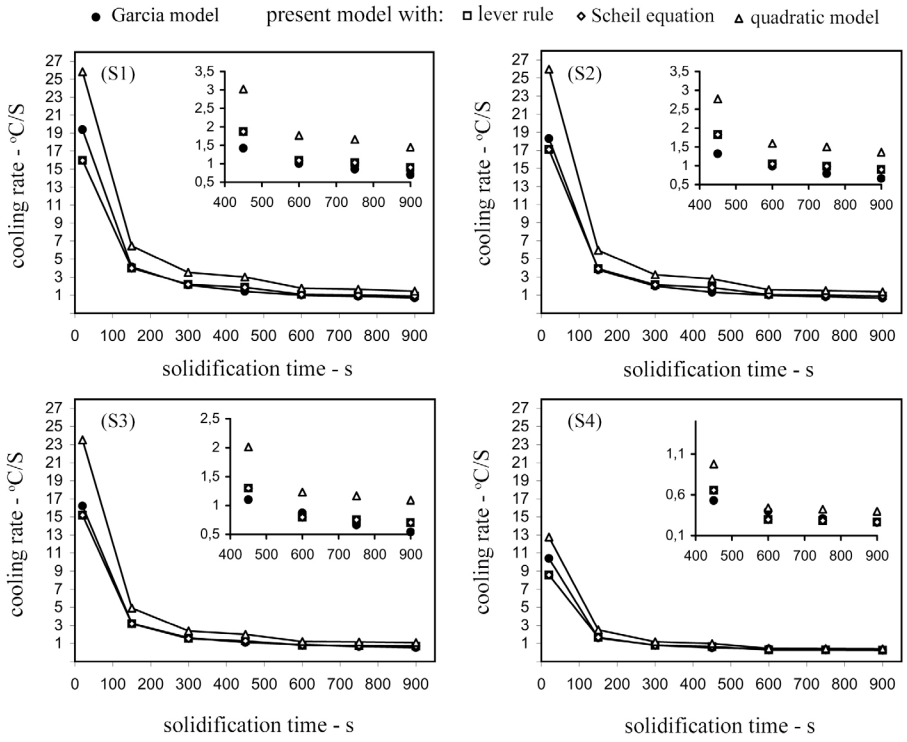

Fig. 9. Comparison of the cooling rates calculated by both SACR and Garcia's models

Acknowledgment

The authors would like to acknowledge the authorities of the International Center for Science, High Technology and Environmental Sciences for their efforts in providing the financial support for this project. Also, the authors express thanks to the authorities of the Iran Alloy Steel Co. for their efforts in conducting the plant trials.

References

[1] Z. Ma, E. Samuel, A.M.A. Mohamed, A.M. Samuel, F.H. Samuel and H.W. Doty: Mater. Des., 31 (2010), 902.
[2] Z. Li, H. Zhong, Q. Sun, Z. Xu and Q. Zhai: Mater. Sci. Eng., A 506 (2009), 191.
[3] M. Rajabi, M. Vahidi, A. Simchi and P. Davami: Mater. Charact., 60 (2009), 1370.
[4] Z. Tang and W. Stumpf: Mater. Sci. Eng. A., 490 (2008), 391.
[5] R.J. Zhang, Z. He, Y. Wang and W.Q. Jie: J. Mater. Sci., 39 (2004), 6379.
[6] D. G. Eskin and L.K. Suyitno: Prog. Mater. Sci., 49 (2004), 629.
[7] M. Rappaz and W.J. Boettinger; Acta Mater., 47 (1999), 3205.
[8] K.H. Kim, H.N. Han, T.J. Yeo, Y.G. Lee, K.H. Oh and D.N. Lee: *in* Melt Spinning**,** Strip Casting and Slab Casting**,** TMS Annual meeting, Anaheim California, Feb. 4–8 (1996), 87.
[9] H. D. Brody and M. C. Flemings: Trans. Metall. Soc. AIME, 236 (1966), 615.
[10] A. Yazdipour, A. Shafiei M and K. Dehghani: Mater. Sci. Eng., A. 27 (2009), 192.
[11] F. Qiu, P. Shen, T. Liu, D. Zhang and Q. Jiang: J. Alloys Compd., 477 (2009), 840.
[12] S. Bontha, N. W. Klingbeil, P. A. Kobryn and H. L. Fraser: J. Mater. Process. Technol., 178 (2006), 135.
[13] F. Sá, O. L. Rocha, C. A. Siqueira and A. Garcia: Mater. Sci. Eng., A. 373 (2004), 131.
[14] C.A, Muojekwu, I.V. Samarasekera and J.K. Brimacombe: Metall. Mater. Trans., B 26 (1995), 361.
[15] H.S. Kim, Y. Kobayashi, S. Tsukamoto and K. Nagai: Mater. Sci. Eng., A 403 (2005), 311.
[16] M.F. Zhu, C.P. Hong, D.M. Stefanescu and Y.A. Chang: Metall. Mater. Trans. B, 38 (2007), 517.
[17] G. A. Santos, C. M. Neto, W. R. Oso´rio and A. Garcia: Mater. Des., 28 (2007), 2425.
[18] W. R. Oso´rio and A. Garcia: Mater. Sci. Eng., A 325 (2002), 103.
[19] O. L. Rocha, C. A. Siqueira and A. Garcia: Mater. Sci. Eng., A 361 (2003), 111.
[20] T. Emi and H. Fredriksson: Mater. Sci. Eng., A 413-414 (2005), 2.
[21] M. Alizadeh, A. Jenabali Jahromi and O. Abouali: Comput. Mater. Sci., 44 (2008), 807.
[22] T.A. Blase, Z.X. Guo, Z. Shi, K. Long and W.G. Hopkins: Mater. Sci. Eng., A 365 (2004), 318.

[23] C.A.Santos, J.A.Spim, M.C.F.Ierardi and A. Garcia: Appl. Math. Model., 26 (2002), 1077.
[24] S. Louhenkilpi, J. Miettinen and L. Holappa: ISIJ Int., 46 (2006), 914.
[25] S. Qiu, H. Liu, S. Peng and Y. Gan: ISIJ Int., 44 (2004), 1376.
[26] H. Wang, G. Li, Y. Lei, Y. Zhao, Q. Dai and J. Wang: ISIJ Int., 45 (2005), 1291.
[27] R. A. Hardin, K. Liu, A. Kapoor and C. Beckermann: Metall. Mater. Trans., B 34 (2003), 297.
[28] G.H. Geiger and D.R. Poirier: Transport phenomena in metallurgy, Addison-Wesley, United States of America, (1973).
[29] Y. Meng and B.G. Thomas: Metall. Mater. Trans., B 34 (2003), 707.
[30] W. Kurz and D. J Fisher: Fundamentals of Solidification, Trans Tech, Switzerland, (1986).
[31] A.M. Mullis: J. Mater. Sci., 38 (2003), 2517.
[32] C.A. Santos, J.A. Spim and A. Garcia: Eng. Appl. Artif. Intell., 16 (2003), 511.